Diagn Interv Radiol DOI 10.5152/dir.2022.20872

ABDOMINAL IMAGING

ORIGINAL ARTICLE

Distinguishing T1-2 and T3a tumors of rectal cancer with texture analysis and functional MRI parameters

Danqi Sun
Xiaojuan Wu
Linghua Wang
Guangzheng Li
Jingyu Huang
Yonggang Li

PURPOSE

We aimed to investigate whether the texture analysis and functional magnetic resonance imaging (fMRI) could differentiate rectal cancer pathological stages T1-2 (pT1-2) and T3a (pT3a).

METHODS

Eighty-two rectal adenocarcinoma patients at stage pT1-2 and pT3a received T2 and fMRI examination before surgery. The latter included apparent diffusion coefficient (ADC) sequence, dynamic contrast enhancement (DCE) MRI, and intravoxel incoherent motion (IVIM) diffusion weighted imaging. Patients were grouped into early stage (pT1-2) and advanced stage (pT3a). The MRI accuracy in diagnosing rectal cancer before surgery was calculated. The differences in clinicopathological variables, quantitative parameters including ADC values, IVIM parameters (perfusion fraction [f], true diffusion coefficient [D], and pseudo-diffusion coefficient [D*]), DCE MRI parameters (transfer constant [K^{trans}], reflux constant [K_{ep}], and extravascular extracellular fractional volume [V_e]), and texture features were compared between the groups. Receiver operating characteristic (ROC) curves of texture features and fMRI parameters were generated to distinguish pT1-2 and pT3a tumors. The multivariate analysis was used to develop a predictive model and to find independent risk factors. Hosmer–Lemeshow test was used to see the fitness of the model. DeLong test was applied to compare the ROC curves of different features. Correlation of texture features and fMRI parameters with stage were calculated using *r* (Spearman's rank correlation coefficient).

RESULTS

The preoperative accuracy in differentiating pT1-2 from pT3a rectal cancer using MRI was 74.39%. K_{ep}, V_e, and ADC showed significant differences between the groups. K_{ep} and ADC showed negative correlation with stage. V_e correlated positively with stage. Twenty-five texture features from T2 images showed significant differences between groups, and S(0,2)SumOfSqs and WavEnLH_s_2 among these showed better performance, showing negative correlation with stage. The area under the curve (AUC) values of S(0,2)SumOfSqs, WavEnLH_s_2, ADC, K_{ep}, and V_e were 0.721, 0.699, 0.690, 0.666, and 0.653, respectively. The multivariate analysis showed that S(0,2) SumOfSqs, WavEnLH_s_2, and ADC are risk factors for advanced tumors, and the logistic model built by K_{ep}, V_e, S(0,2)SumOfSqs, WavEnLH_s_2, and ADC has the AUC, sensitivity, and specificity of 0.833, 88.5%, and 73.3%, respectively. ROC curve of the model showed statistical significance between S(0,2)SumOfSqs, ADC, K_{ep}, and V_e. The *P* value of the Hosmer–Lemeshow test was 0.65.

CONCLUSION

S(0,2)SumOfSqs, WavEnLH_s_2, and ADC are risk factors for advanced rectal cancer, and the model built by K_{ep}, V_e, S(0,2)SumOfSqs, WavEnLH_s_2, and ADC has better performance than using a single method. The application of above combinations could be beneficial to patients' accurate and individualized treatments.

Department of Radiology (J.H. suzhouzhuoma@163.com, Y.L. liyonggang224@163.com), The First Affiliated Hospital of Soochow University, Suzhou, China.

Received 25 October 2020; revision requested 23 November 2020; last revision received 14 April 2021; accepted 28 April 2021.

Published online 22 April 2022.

DOI: 10.5152/dir.2022.20872

Patients with early stages of rectal cancer (T1-2) still have the opportunity to receive organ-preserving surgical treatment.[1] According to previous research studies,[2,3] neoadjuvant chemoradiotherapy (NCRT) has become essential treatment strategy of great necessity for patients with advanced rectal cancer (T3-4) to improve disease-free survival. This is because patients with advanced rectal cancer have more probability of local recurrence and distant metastasis than those with the early stage of rectal cancer. Magnetic resonance imaging (MRI) has been used for tumor diagnosis due to its extra-ordinary soft tissue resolution, and clear observation of in depth and extent of tumor

You may cite this article as: Sun D, Wu X, Wang L, Li G, Huang J, Li Y. Distinguishing T1-2 and T3a tumors of rectal cancer with texture analysis and functional MRI parameters. *Diagn Interv Radiol*. 2022;28(3):200-207

invasion as a whole, when compared to endoscope or biopsies that present the lesion with limited view and information.[4] However, MRI staging of rectal cancer largely depends on T2 images in the current clinical practice.[5] It has been reported that pre-operative MRI staging often leads to overstaging,[6] which is frequently seen in distinguishing T2 and small T3 tumors of rectal cancer,[7] resulting in unsatisfying specificity in diagnosing T3 tumors. This leads to the use of unnecessary NCRT treatments and aggressive surgeries to patients. Previous researches[8,9] revealed that overstaging is mostly caused due to edema, inflammatory and desmoplastic reactions, and penetration of small vessels into the walls, while understaging partially results from infiltration of mesorectal fat. Above all, there is an urgent need for a better staging method before surgery. Previous study[10] has revealed some limitations of MRI in differentiating T1 and T2 stage tumors when compared to endoscopic ultrasound. Taking the limitations of MRI in diagnosing T1 and T2 tumors and the similar treatments to T1-2 patients into consideration, T1-2 patients were enrolled into the early stage group. Functional MRI (fMRI), which includes apparent diffusion coefficient (ADC) imaging, dynamic contrast enhancement (DCE), and intravoxel incoherent motion (IVIM) MRI, could provide more information about the tumors' biological behavior before surgery. ADC maps reflect the water content and cellularity,[11] which indicates tumor aggressiveness. IVIM estimates the perfusion and diffusivity of the tumor separately by using different b values, and its parameters of true-diffusion coefficient (D), pseudo-diffusion coeffient (D*), and perfusion fraction (f) can provide microvessel density information of the tumor.[12] Thus, IVIM has now been widely used for evaluating the tumors' microstructure, microcirculation, response to NCRT in correlation with pathological results. DCE MRI has similar application as IVIM and is regarded as a perfusion-related method whose parameters transfer constant (K^{trans}), reflux constant (K_{ep}), and extravascular extracellular fractional volume (V_e) reflect the tissues' microcirculation and permeability.[13] Texture analysis is an emerging method that is applied to acquire quantitative information of various diseases and serves as an imaging biomarker to better understand tumors' behavior. Previous study[14] has revealed that texture parameters were correlated with tumor hypoxia and angiogenesis. Nowadays, texture analysis has been widely used for evaluating NCRT efficacy, lymph node metastasis, long-term survival in rectal cancer patients, and so on. But to the best of our knowledge, no articles were found investigating the performance of these methods in differentiating rectal cancer between pT1-2 and pT3a. Most of the researches[15,16] have included only MR morphological features, clinicopathological information into texture analysis, or purely analyzed functional parameters' correlation with biological behavior. As a result, we aimed to find out their performance in staging rectal cancer.

Main points

- Texture features and functional magnetic resonance imaging (fMRI) parameters are able to distinguish T3a from early stage tumors of rectal cancer.
- S(0,2)SumOfSqs, WavEnLH_s_2, reflux constant (K_{ep}), and apparent diffusion coefficient (ADC) correlate negatively, while extravascular extracellular fractional volume (V_e) correlates positively with tumor stage.
- S(0,2)SumOfSqs, WavEnLH_s_2, and ADC are risk factors for advanced rectal cancer, and the model built by K_{ep}, V_e, S(0,2) SumOfSqs, WavEnLH_s_2, and ADC has satisfying performance in predicting T3a tumors, compared with single parameters.
- The combined application of texture analysis and fMRI is able to provide quantitative information before surgery and improve the preoperative diagnosis accuracy.

Methods

Patients

This study was approved by the ethics committee of the institution (2020093), and informed consent was waived because of the retrospective nature of the study. A total of 118 patients pathologically diagnosed with rectal adenocarcinoma after surgery from 2016 to 2019 were retrospectively reviewed. After excluding patients with incomplete clinicopathological data, fMRI sequences, poor image quality, and NCRT treatment before examination, 82 patients were finally enrolled in this study (Figure 1). Among these, 30 patients were at early stage of tumor (pT1-2), and the remaining 52 patients had advanced rectal adenocarcinoma (pT3a). Clinicopathological and MRI information (Table 1) that could be acquired before surgery were chosen for the analysis, including sex, age, and differentiation.

MRI examination

For all patients, 3.0 Tesla MRI examination with 16-channel phased-array body coil (Magnetom Skyra 3.0T, Siemens Healthcare) was performed. All patients obtained contrast injection with a dosage of 0.2 mL/kg (Gd-DTPA, Magnivest, Bayer Schering Pharma) at a rate of 3 mL/s. Representative MRI images are presented in Figure 2.

Acquisition of fMRI parameters and texture features

The evaluation of IVIM and DCE MRI parameters and the acquisition of texture features were done by two radiologists. Out of the consideration that tumor stage representing only the farthest distance it invades and being as static histological variable denoting its growing condition, ROIs were eventually delineated on the largest cross-sectional area on T2 images for quantitative parameters better reflecting the tumor stage. The largest cross-sectional area was determined by two observers' negotiation according to the longest diameter of the tumor. For these functional parameters and texture features, two radiologists have manually drawn the regions of interest (ROIs) along the border of tumor and avoided necrosis, water, and hemorrhage and avoided controversial borders. The ROIs of DCE were drawn on axial T2 images and then were automatically copied to DCE images to generate corresponding parameters by using Tissue 4D (Siemens Healthcare) with Tofts model, AIF:FAST mode. ADC values were measured on the workstation of Magnetom Skyra 3.0T (Siemens Healthcare), and IVIM parameters were acquired by using MITK-diffusion software (version 4.13.2, https://github.com/MIC-DKFZ/MITK-Diffusion). Finally, MaZda (version 4.7, https://www.Eletel.p.Lodz.Pl/mAzda/, Institute of Electronics, Technical University of Lodz) was used to achieve the texture features. Before delineation, all images have received normalization of their pixels to $\mu \pm 3\sigma$,[17] and then, ROIs were drawn on T2 images. This resulted in the eventual

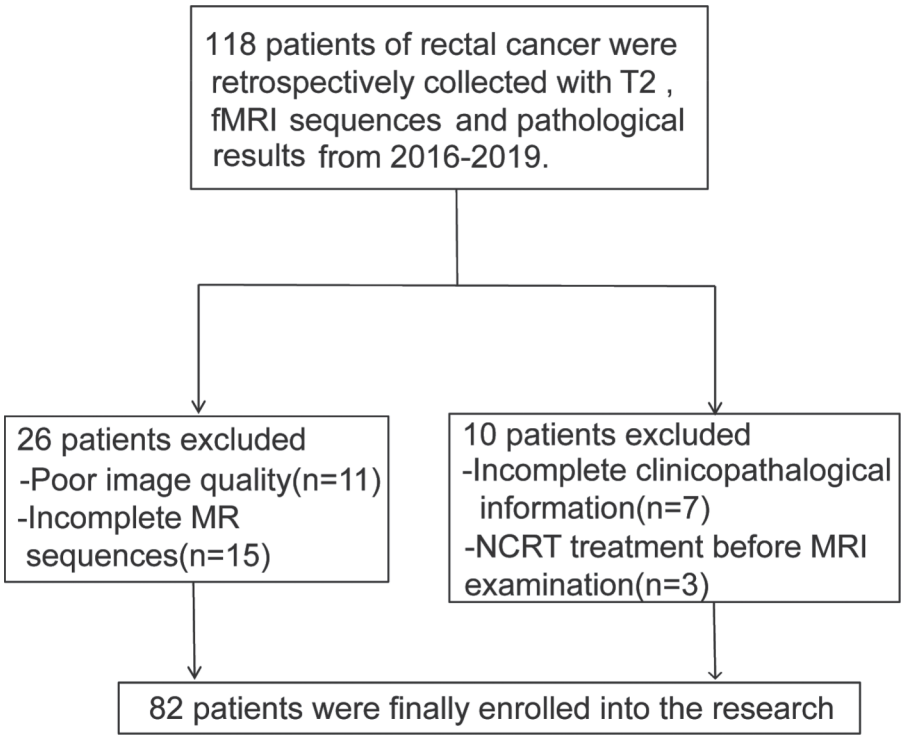

Figure 1. Flow diagram of patients diagnosed with rectal cancer.

generation of 295 texture features and could be categorized into histogram features, gradient-based features, run-length matrix-based parameters, co-occurrence matrix-derived parameters, autoregressive model parameters, and wavelet features. More information about these features were demonstrated in a previous study.[18] and could be found in the supplementary information (Table S1 and Supplementary part 2).

Histopathologic extramural invasion evaluation

A pathologist who was blinded to patients' information measured the tumors' maximum invasion distance into mesorectal fat on the specimens. Finally, patients at T1-2 stage (without extramural invasion) and T3a stage (extramural spread distance <5 mm) were selected into analysis.

Statistical analysis

Statistical analyses were processed by R Studio (version1.1.463, https://www.r-project.org) and TBtools (version0.6733,

Table 1. Clinicopathological, functional magnetic resonance imaging (fMRI), and texture features of patients between groups

	T1-2	T3a	*P*
Total, n (%)	30 (37)	52 (63)	0.77
Age (years), mean ± SD	63.07 ± 9.42	62.37 ± 11.22	
Sex, n (%)			
Male	18 (60)	32 (62)	0.89
Female	12 (40)	20 (38)	
Differentiation, n (%)			
Well	0 (0)	0 (0)	0.38
Medium	26 (87)	41 (79)	
Poor	4 (13)	11 (21)	
K^{trans}(min^{-1}), mean ± SD	0.18 ± 0.04	0.20 ± 0.12	0.80
K_{ep}(min^{-1}), mean ± SD	1.24 ± 0.48	1.03 ± 0.72	0.013
V_e, mean ± SD	0.18 ± 0.08	0.21 ± 0.07	0.022
f, mean ± SD	0.15 ± 0.07	0.18 ± 0.14	0.50
D ($10^{-3}mm^2{\cdot}s^{-1}$), mean ± SD	0.97 ± 0.31	0.98 ± 0.24	0.30
D* ($10^{-3}mm^2{\cdot}s^{-1}$), mean ± SD	7.51 ± 3.04	8.59 ± 2.59	0.076
ADC ($10^{-3}mm^2{\cdot}s^{-1}$), mean ± SD	995.34 ± 189.84	893.44 ± 115.94	0.004
S(0,2)SumOfSqs, mean ± SD	117.00 ± 32.51	91.41 ± 28.65	0.000
WavEnLH_s_2, mean ± SD	235.16 ± 158.75	163.88 ± 116.12	0.003

SD, standard deviation; K^{trans}, transfer constant; K_{ep}, reflux constant; V_e, extravascular extracellular fractional volume; f, perfusion fraction; D, true diffusion coefficient; D*, pseudo-diffusion coefficient; ADC, apparent diffusion coefficient.

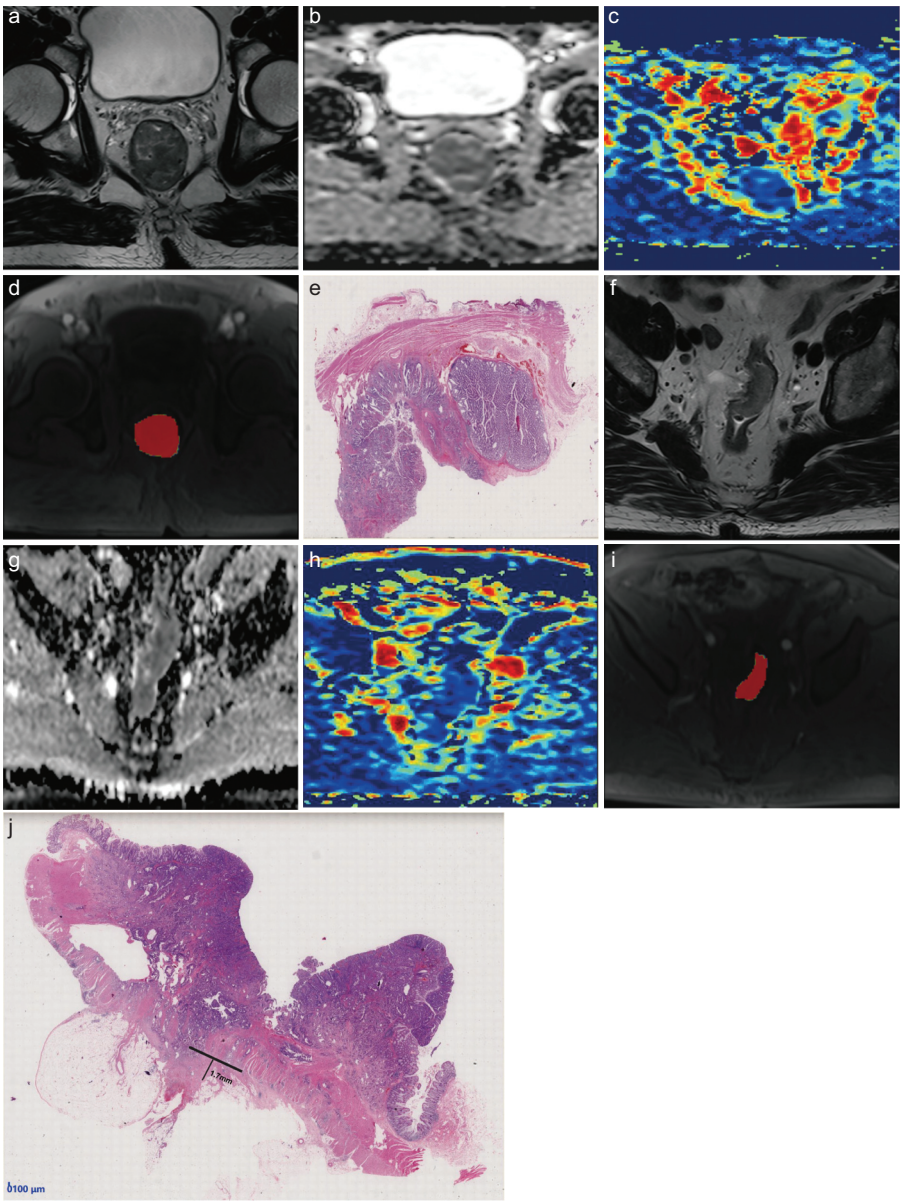

Figure 2. a-j. Panels **(a-e)** show: **(a)**, T2 image; **(b)**, apparent diffusion coefficient (ADC) map; **(c)**, pseudo-color image of perfusion fraction (f); **(d)**, pseudo-color image of reflux constant (K_{ep}); **(e)**, pathological image from a T2 stage patient (H&E, ×20). Panels **(f-j)** show:**(f)**, T2 image; **(g)**, ADC map; **(h)**, pseudo-color image of f; **(i)** pseudo-color image of K_{ep}; **(j)**,pathological image from a T3a stage patient (H&E, ×20). The *black line* in **(j)** shows the extramural invasion distance from the baseline of muscle layer, which is 1.7 mm.

https://github.com/CJ-Chen/TBtools). Intraclass correlation coefficient (ICC) was applied to test inter-observer and intra-observer reliabilities. The features with values >0.70 were included.[19] Levene's test and Kolmogorov–Smirnov test were used to identify the homogeneity and normality of numeric variances. If numeric variances are normal (P_K > .05) and homogeneous (P_L > 0.050), then independent *t* test was applied to find out the significance (P_T < .05) between the two groups. Mann–Whitney *U*-test was used to analyze the significance (P_U < .05) of categorical variables and numeric parameters that could not meet the above standard. To find out the correlation between texture features, DCE parameters, and stage (categorized as early and advanced stage), Spearman's test was used, as pre-operative acquired parameters were intended to enroll into receiver operating characteristic (ROC) analysis and to find their predictive performance. Multivariate logistic regression analysis was used with entry of variables to identify predictors of advanced rectal cancer and to develop a predictive model. Hosmer–Lemeshow test was used to see the fitness of the model. Finally, respective ROC curve of texture features and functional parameters were generated. DeLong test was applied to find out the difference between ROC curves.

Results

Inter- and intraobserver ICC of ADC, DCE, and IVIM parameters were shown to be >0.70. The accuracy in differentiating pT1-2 from pT3a rectal cancer using MRI before surgery was 74.39%. K_{ep}, V_e, and ADC showed significant differences between the groups: P_{Kep} = .013, P_{Ve} = .022, and P_{ADC} = .004 (Table 1). Twenty-five texture features with inter and intra-observer ICC >0.70 showed statistically significant differences. ICC of 25 texture features and functional parameters with significance between groups are found in Table S2. The categorized features are listed in Table 2. Two texture features of S(0,2)SumOfSqs and WavEnLH_s_2 displayed the best performance in staging (P_T = .000, P_U = .003). The results of Spearman correlation test of S(0,2)SumOfSqs, WavEnLH_s_2 with K_{ep}, V_e, ADC, and pathological stage (grouped as pT1-2 [early stage] and pT3a [advanced tumor]) are presented in Figure 3. The results revealed that K_{ep} and ADC had negative correlation with stage (r_{Kep} = −0.277, r_{ADC} = −0.318). V_e was positively related to stage (r_{Ve} = 0.255). S(0,2) SumOfSqs and WavEnLH_s_2 had negative correlation with stage (*r* = −0.369, *r* = −0.332). The area under the curve (AUC), sensitivity, and specificity of S(0,2) SumOfSqs, WavEnLH_s_2, ADC, K_{ep}, and V_e are listed in Table 3. The multivariate logistic regression analysis showed that WavEnLH_s_2, S(0,2)SumOfSqs, and ADC are risk factors for advanced rectal cancer in the model. Hosmer–Lemeshow test revealed good fitness (*P* = .65) of the model [y = 8.844-0.032S(0,2)SumOfSqs-0.006WavEnLH_s_2-0.004ADC-0.565K_{ep} + 4.006V_e]. Odds ratio, 95% confidence interval, and *P* value of WavEnLH_s_2, S(0,2)SumOfSqs, and ADC are listed in Table 4. The AUC, sensitivity, and specificity of the model are 0.833, 88.5%, and 73.3% (Table 3). ROC curves are presented in Figure 4.

DeLong test showed significance between ROCs of the model and S(0,2)SumOfSqs, ADC, K_{ep}, and V_e, except for WavEnLH_s_2 (Table 5).

Discussion

Patients with advanced rectal cancer should regularly receive NCRT treatments. However, the pre-operative diagnostic accuracy is restricted by the experience of the observer and imaging condition.[20] It has been reported that the accuracy of predicting the cancer stage of patients by different observers might vary from 67% to 83%,[21] which is in accordance with our pre-operative diagnostic accuracy. This resulted in a quest to find a precise staging method before treatment that differentiates advanced rectal cancer (T3a) from its early stage (T1-2), offering patients the opportunity of receiving individualized and less aggressive treatments. In our study, we found that texture features, K_{ep}, V_e, and ADC values are able to differentiate pT1-2 from pT3a rectal cancer, and their comprehensive application showed the best performance in predicting.

Due to limited number of patients, no statistical significance was observed in IVIM parameters between groups. Previous studies have revealed correlation between IVIM parameters and microvessel and cell density of the tumors. Sun et al.[22] have found that advanced rectal cancer has lower D and D* values. Other studies[23] have reported significant correlation between f and vascular area fraction, f and vascular diameter, and between D*, f, and vessel count.[24]

Our study revealed that K_{ep} and V_e were significantly different between groups. K_{ep} is the rate constant that indicates the transfer between extravascular extracellular space and the blood compartment. V_e stands for the fractional volume of the extravascular and extracellular space. In our study, K_{ep} showed negative correlation with T stage (r_{kep}=-0.277), while V_e correlates positively with stage(r_{Ve}=0.255), and the results were concordant with the study conducted by Chen et al.[25] Their study found that patients with MRI-detected extramural invasion have lower K_{ep} and higher V_e values, and these patients tend to have higher tumor stages. These values revealed that K_{ep} largely depends not only on the permeability but also on the permeability surface area. As considerable number of tumor cells could leak into tumor vessels, this might decrease the surface area, leading to hypoxia and microscopic necrosis, resulting in lower values of K_{ep}. Yeo et al.[26] have found that T1 stage patients have higher K_{ep} than those from T2-4. They also explained that advanced tumor has uneven enhancements due to micronecrosis and hemorrhage, and in contrast, the early stage cancer tends to have more uniform enhancement, both resulting in the offset effect on K_{ep}. Researchers[27] have found that V_e showed a correlation tendency with cell count. Since cell proliferation is more active in advanced tumors, it might result in more tumor cells and higher values of V_e than early stage tumors. However, DCE parameters showed poor performance in staging and poor correlation with stage in our study, and this was in accordance with the study conducted by Kim et al.[28] Studies[26,29] have indicated that DCE parameters might reflect the angiogenic activity of tumors. Angiogenesis is related to tumors' aggressiveness,[30] which can be measured by stage.[31] However, stage is one kind of static histological result that indirectly reflects tumors' angiogenic status. According to a previous study,[32] the DCE parameters do not denote well the static histological angiogenic process of tumors because these parameters are more dynamic and comprehensive in reflecting the vasculature variations, while angiogenesis evaluated by histological methods provides static view and its results vary in different parts of the tumors. Limited number of patients enrolled in this study may as well result in unsatisfying AUC.

Our research also revealed a negative correlation between ADC and tumor stage (r = -0.318). It is well known that ADC values represent the degree of free diffusion restricted by cells,[11] resulting in lower ADC values due to higher cell intensity. Lu et al.[33] have found significant differences between pT1-2 and pT3a, with mean ADC values of $1.110*10^{-3}$ mm^2/s, and $1.030*10^{-3}$ mm^2/s, and the result was consistent with our research. The AUC of ADC was 0.690. According

Table 2. Categorized texture features with statistical significance between groups

Co-occurrence matrix-derived parameters	Wavelet parameters
Correlat	WavEnLH
Contrast	WavEnHL
InvDfMom	WavEnHH
SumEntrp	
SumVarnc	
SumOfSqs	

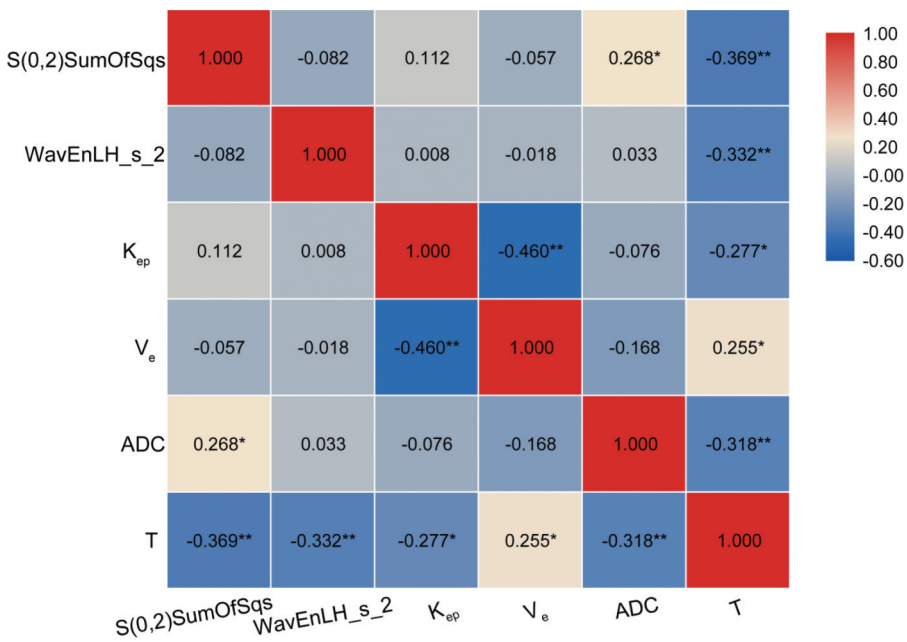

Figure 3. Correlation of functional MRI parameters and texture features with tumor stages (tumor stages were categorized into T1-2 and T3a). K_{ep}, reflux constant; V_e, extravascular extracellular fractional volume; ADC, apparent diffusion coefficient; T, tumors stages categorized into T1-2 and T3a. *P < 0.050. **P < 0.010.

Table 3. Area under the curve (AUC), sensitivity, specificity, and cut-offs of texture features, functional magnetic resonance imaging (fMRI) parameters, and the logistic model

	AUC (95% CI)	Sensitivity (95% CI)	Specificity (95% CI)	Cut-Cutoff
S(0,2)SumOfSqs	0.721 (0.611-0.815)	53.9 (39.5-67.8)	83.3 (65.3-94.4)	93.76
WavEnLH_s_2	0.699 (0.587-0.795)	59.6 (45.1-73.0)	76.7 (57.7-90.1)	148.18
K_{ep}	0.666 (0.553-0.766)	50.0 (35.8-64.2)	83.3 (65.3-94.4)	0.89
V_e	0.653 (0.539-0.754)	53.9 (39.5-67.8)	73.3 (54.1-87.7)	0.19
ADC	0.690 (0.579-0.788)	90.4 (79.0-96.8)	53.3 (34.3-71.7)	960.17
Model	0.833 (0.735-0.907)	88.5 (76.6-95.6)	73.3 (54.1-87.7)	0.56

The logistic model is defined as $y = 8.844\text{-}0.032S(0,2)SumOfSqs\text{-}0.006WavEnLH\_s\_2\text{-}0.004ADC\text{-}0.565K_{ep} + 4.006V_e$. CI, confidence interval; ADC, apparent diffusion coefficient; K_{ep}, reflux constant; V_e, extravascular extracellular fractional volume.

Table 4. Independent risk factors from the logistic regression model in predicting pT3a rectal cancer

Variance	OR	95% CI	*P*
S(0,2)SumOfSqs	0.968	0.949-0.988	0.002
WavEnLH_s_2	0.994	0.989-0.998	0.008
ADC	0.996	0.992-1.000	0.032

OR, odds ratio; CI, confidence interval; ADC, apparent diffusion coefficient.

to Chen et al.,[34] the best combination of b values is 0 and 1000, and AUC of these could reach to 0.901, with good repeatability. From our point of view, due to limited number of enrolled patients, which is coupled with different combination of b values (b = 0, 800), the ADC values in our study showed no excellent AUC performance.

In our study, second-order texture feature S(0,2)SumOfSqs from gray-level co-occurrence matrix (GLCM) and WavEnLH_s_2 from wavelet parameters have moderate ability to differentiate T stages of rectal cancer, with AUC values of 0.721 and 0.699, respectively, and their joint AUC was 0.795. Both S(0,2)SumOfSqs and WavEnLH_s_2 showed negative correlation with pathological stage. S(0,2)SumOfSqs showed positive correlation with ADC values, indicating their possible ability to reflect the inhomogeneity of the images. Fang et al.[35] have found that patients with lymph node metastases have lower values of WavEnLH_s-2 when compared to the negative group, which is in accordance with our results. Wavelet parameters are acquired after discrete wavelet transform (DWT), decomposing the data into various frequency components, and the resolution of aimed components was matched according to their scale. WavEnLH_s_2 means that wavelet energy of rows and columns is filtered through low-pass and high-pass bands with a scale factor of 2. We considered that DWT is capable of detecting the structures of the images, especially those that are not visible, and then might show tumor heterogeneity. SumOfSqs measures the distribution of neighboring intensity level pairs with respect to the average intensity level in GLCM. As to S(0,2)SumOfSqs, Yan et al.[36] have found that high-grade meningiomas have higher S(2,2)SumOfSqs values, which is not in-line with our results. It is worth mentioning that Meyer et al.[37] have found that S(1,0)Diffvarnc, S(2,0)Diffvarnc, and S(4,0)Diffvarnc showed negative correlation with Ki-67 on T2 images, while S(3,0)Diffvarnc showed positive correlation with Ki-67. This could be explained by the fact that tumors reveal heterogeneity in different parts, and this kind of heterogeneity is finally expressed in different areas of images. We suppose that the heterogeneity of tumors cannot be solely explained based on the type of features, but the changes brought by different regions in tumors and the performance of these features in specific areas with certain distances or directions between voxel pairs must also be considered.

We noticed that the second-order features and wavelet parameters showed better performance in differentiating rectal cancer than ADC values. GLCM features estimated the joint probability of the presence of the two neighboring pixels' in images, while wavelet parameters are able to amplify the subtle intensity variation and to reflect the intensity inhomogeneity inside the tumor areas. Both can better reflect the heterogeneity or homogeneity in tumors, while ADC values reflect average gray scale of all voxels, without taking the pixels' higher dimensional relationship into consideration. For example, Liu et al.[38] also found that GLCM features perform better than histogram features from first-order in predicting the pathological response after chemoradiotherapy. However, GLCM and wavelet parameters only provide second order and transformed information of images; then, ADC values (gray-level related parameter) and DCE parameters (reflecting tumors' microcirculation) were included in order to observe more comprehensive performance in differentiating rectal cancer. The multivariate analysis shows that S(0,2)SumOfSqs, WavEnLH_s_2, and ADC are risk factors for advanced rectal cancer in the model. The logistic model built by K_{ep}, V_e, S(0,2)SumOfSqs, WavEnLH_s_2, and ADC showed a moderate AUC of 0.833, a sensitivity of 88.5%, and a specificity of 73.3%. The ROC curve of the model is statistically significantly different compared with the ROC curves of S(0,2)SumOfSqs, K_{ep}, V_e, and ADC, respectively. Although the difference between the ROC curve of the model and WavEnLH_s_2 is not statistically significant, the former one shows better sensitivity in predicting. The model indicates that combine application of texture analysis and fMRI can provide quantitative information before surgery and make up for the shortcomings of using a single parameter or a single method in pre-operative diagnosis. In the long run, joint application of multiple technologies could compensate for the deviations caused

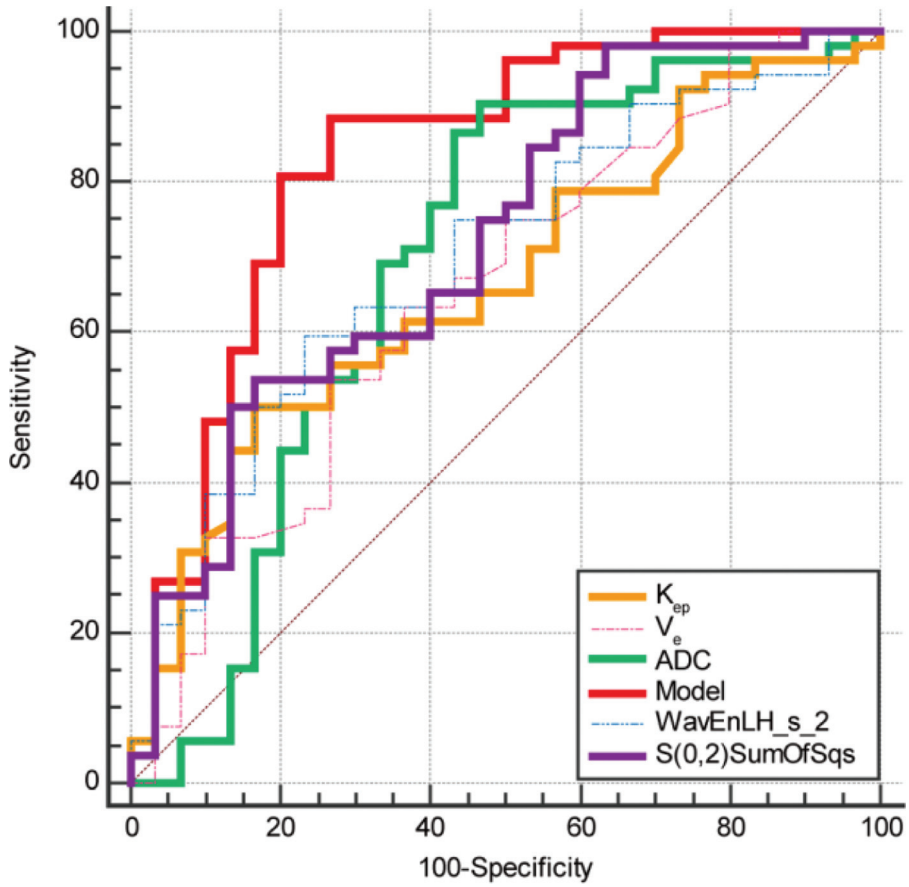

Figure 4. Receiver operating characteristic (ROC) curve of S(0,2)SumOfSqs, WavEnLH_s_2, reflux constant (K_{ep}), extravascular extracellular fractional volume (V_e), apparent diffusion coefficient (ADC) and the logistic regression model: y = 8.844-0.032S(0,2)SumOfSqs-0.006WavEnLH_s_2-0.004ADC-0.565K_{ep} + 4.006V_e.

Table 5. Results of DeLong test between the model and different features

Model VS texture feature or functional parameters	*P*	95% CI
Model VS S(0,2) SumOfSqs	0.0292	0.0114-0.213
Model VS WavEnLH_s_2	0.0638	–0.00772-0.277
Model VS ADC	0.0054	0.0422-0.244
Model VS K_{ep}	0.0208	0.0255-0.310
Model VS V_e	0.0094	0.0443-0.317

The logistic model is defined as y = 8.844-0.032S(0,2)SumOfSqs-0.006WavEnLH_s_2-0.004ADC-0.565K_{ep} + 4.006V_e.
K_{ep}, reflux constant;
V_e, extravascular extracellular fractional volume; CI, confidence interval; ADC, apparent diffusion coefficient.

by doctors' experience and significantly improve the diagnostic performance.

However, our research still has some limitations that should be acknowledged. First, the number of enrolled patients is limited. Since this is a preliminary research of radiomics in differentiating T1-2 from T3a tumors, we plan to enroll more patients in the future for model development and validation. Moreover, the reproducibility of functional parameters acquired by various software might vary,[39] and the texture features could be influenced by pre- and post-processing methods. Also, different parameter settings of MRI sequences might influence the final results. Finally, multi-center researches are needed to verify the findings of our study, and more studies are warranted to investigate the specific meaning of features in certain regions and to find out the differences between various areas.

In conclusion, S(0,2)SumOfSqs, WavEnLH_s_2, ADC, K_{ep}, and V_e of tumors before treatment can, respectively, assist in differentiating pT1-2 patients from pT3a, and the model built by them has better performance in predicting tumor stage compared with single texture features or fMRI parameters, with S(0,2) SumOfSqs, WavEnLH_s_2, and ADC determined as risk factors for advanced tumors. Above all, the comprehensive use of these methods in clinical practice is advised.

Acknowledgments

This work received the support of Weishuo Liu from the Department of Pathology of the First Affiliated Hospital of Soochow University.

Conflict of interest disclosure

The authors declared no conflicts of interest.

Financial disclosure

This work was supported by the Technological Innovation Project of Suzhou Jiangsu Province [grant number SYS201734], Suzhou Clinical Key Diseases Diagnosis and Treatment Technology Special Project [grant number LCZX 201801], Six-one Project for High-level Health Talents in Jiangsu Province [grant number LGY2016035], and the National Natural Science Foundation of China [grant number 81671743].

References

1. Balyasnikova S, Brown G. Optimal imaging strategies for rectal cancer staging and ongoing management. *Curr Treat Options Oncol*. 2016;17(6):32. [Crossref]
2. DeSantis CE, Lin CC, Mariotto AB, et al. Cancer treatment and survivorship statistics, 2014. *CA Cancer J Clin*. 2014;64(4):252-271. [Crossref]
3. Ludmir EB, Palta M, Willett CG, Czito BG. Total neoadjuvant therapy for rectal cancer: An emerging option. *Cancer*. 2017;123(9):1497-1506. [Crossref]
4. Palmucci S, Piccoli M, Piana S, et al. Diffusion MRI for rectal cancer staging: ADC measurements before and after ultrasonographic gel lumen distension. *Eur J Radiol*. 2017;86:119-126. [Crossref]
5. Horvat N, Carlos Tavares Rocha C, Clemente OB, Petkovska I, Gollub MJ. MRI of rectal cancer: Tumor staging, imaging techniques, and management. *Radiographics*. 2019;39(2):367-387. [Crossref]
6. Danihel LJr., Danihel LSr., Rajcok M, et al. Significance of MRI in rectal carcinoma therapy optimization - correlation of preoperative T- and N-staging with definitive histopathological findings. *Neoplasma*. 2019;66(3):494-498. [Crossref]
7. Taylor FG, Swift RI, Blomqvist L, Brown G. A systematic approach to the interpretation of preoperative staging MRI for rectal cancer. *AJR Am J Roentgenol*. 2008;191(6):1827-1835. [Crossref]
8. Laghi A, Ferri M, Catalano C, et al. Local staging of rectal cancer with MRI using a phased array body coil. *Abdom Imaging*. 2002;27(4):425-431. [Crossref]

9. Hoeffel C, Mule S, Laurent V, Bouche O, Volet J, Soyer P. Primary rectal cancer local staging. *Diagn Interv Imaging*. 2014;95(5):485-494. [Crossref]
10. Boot J, Gomez-Munoz F, Beets-Tan RGH. Imaging of rectal cancer. *Radiologe*. 2019;59(Suppl 1):46-50. [Crossref]
11. Sun Y, Tong T, Cai S, Bi R, Xin C, Gu Y. Apparent Diffusion Coefficient (ADC) value: A potential imaging biomarker that reflects the biological features of rectal cancer. *PLoS One*. 2014;9(10): e109371. [Crossref]
12. Surov A, Meyer HJ, Hohn AK, et al. Correlations between intravoxel incoherent motion (IVIM) parameters and histological findings in rectal cancer: Preliminary results. *Oncotarget*. 2017;8 (13):21974-21983. [Crossref]
13. Gurses B, Boge M, Altinmakas E, Balik E. Multiparametric MRI in rectal cancer. *Diagn Interv Radiol*. 2019;25(3):175-182. [Crossref]
14. Ganeshan B, Goh V, Mandeville HC, Ng QS, Hoskin PJ, Miles KA. Non-small cell lung cancer: Histopathologic correlates for texture parameters at CT. *Radiology*. 2013;266(1):326-336. [Crossref]
15. Liang C, Huang Y, He L, et al. The development and validation of a CT-based radiomics signature for the preoperative discrimination of stage I-II and stage III-IV colorectal cancer. *Oncotarget*. 2016;7(21):31401-31412. [Crossref]
16. Liu L, Liu Y, Xu L, et al. Application of texture analysis based on apparent diffusion coefficient maps in discriminating different stages of rectal cancer. *J Magn Reson Imaging*. 2017;45(6):1798-1808. [Crossref]
17. Larue R, Van Timmeren JE, De Jong EEC, et al. Influence of gray level discretization on radiomic feature stability for different CT scanners, tube currents and slice thicknesses: A comprehensive phantom study. *Acta Oncol*. 2017;56(11):1544-1553. [Crossref]
18. Szczypinski PM, Strzelecki M, Materka A, Klepaczko A. MaZda—A software package for image texture analysis. *Comput Methods Programs Biomed*. 2009;94(1):66-76. [Crossref]
19. Yang L, Liu D, Fang X, et al. Rectal cancer: Can T2WI histogram of the primary tumor help predict the existence of lymph node metastasis? *Eur Radiol*. 2019;29(12):6469-6476. [Crossref]
20. Pedersen BG, Blomqvist L, Brown G, Fenger-Gron M, Moran B, Laurberg S. Postgraduate multidisciplinary development program: Impact on the interpretation of pelvic MRI in patients with rectal cancer: A clinical audit in West Denmark. *Dis Colon Rectum*. 2011;54 (3):328-334. [Crossref]
21. Beets-Tan RG, Beets GL, Vliegen RF, et al. Accuracy of magnetic resonance imaging in prediction of tumour-free resection margin in rectal cancer surgery. *Lancet*. 2001;357(9255):497-504. [Crossref]
22. Sun H, Xu Y, Song A, Shi K, Wang W. Intravoxel incoherent motion mri of rectal cancer: Correlation of diffusion and perfusion characteristics with prognostic tumor markers. *AJR Am J Roentgenol*. 2018;210(4): W139-W147. [Crossref]
23. Lee HJ, Rha SY, Chung YE, et al. Tumor perfusion-related parameter of diffusion-weighted magnetic resonance imaging: Correlation with histological microvessel density. *Magn Reson Med*. 2014;71(4):1554-1558. [Crossref]
24. Bauerle T, Seyler L, Munter M, et al. Diffusion-weighted imaging in rectal carcinoma patients without and after chemoradiotherapy: A comparative study with histology. *Eur J Radiol*. 2013;82(3):444-452. [Crossref]
25. Chen Y, Yang X, Wen Z, et al. Association between high-resolution MRI-detected extramural vascular invasion and tumour microcirculation estimated by dynamic contrast-enhanced MRI in rectal cancer: Preliminary results. *BMC Cancer*. 2019;19(1):498. [Crossref]
26. Yeo DM, Oh SN, Jung CK, et al. Correlation of dynamic contrast-enhanced MRI perfusion parameters with angiogenesis and biologic aggressiveness of rectal cancer: Preliminary results. *J Magn Reson Imaging*. 2015;41(2):474-480. [Crossref]
27. Surov A, Meyer HJ, Gawlitza M, et al. Correlations between DCE MRI and histopathological parameters in head and neck squamous cell carcinoma. *Transl Oncol*. 2017;10(1):17-21. [Crossref]
28. Kim YE, Lim JS, Choi J, et al. Perfusion parameters of dynamic contrast-enhanced magnetic resonance imaging in patients with rectal cancer: Correlation with microvascular density and vascular endothelial growth factor expression. *Korean J Radiol*. 2013;14 (6):878-885. [Crossref]
29. Hong HS, Kim SH, Park HJ, et al. Correlations of dynamic contrast-enhanced magnetic resonance imaging with morphologic, angiogenic, and molecular prognostic factors in rectal cancer. *Yonsei Med J*. 2013;54(1):123-130. [Crossref]
30. Miao H, Ruan S, Shen M. VEGF-C in rectal cancer tissues promotes tumor invasion and metastasis. *J BUON*. 2018;23(1):42-47.
31. Dijkhoff RAP, Beets-Tan RGH, Lambregts DMJ, Beets GL, Maas M. Value of DCE-MRI for staging and response evaluation in rectal cancer: A systematic review. *Eur J Radiol*. 2017;95:155-168. [Crossref]
32. Atkin G, Taylor NJ, Daley FM, et al. Dynamic contrast-enhanced magnetic resonance imaging is a poor measure of rectal cancer angiogenesis. *Br J Surg*. 2006;93(8):992-1000. [Crossref]
33. Lu ZH, Hu CH, Qian WX, Cao WH. Preoperative diffusion-weighted imaging value of rectal cancer: Preoperative T staging and correlations with histological T stage. *Clin Imaging*. 2016;40 (3):563-568. [Crossref]
34. Chen L, Shen F, Li Z, et al. Diffusion-weighted imaging of rectal cancer on repeatability and cancer characterization: An effect of b-value distribution study. *Cancer Imaging*. 2018;18 (1):43. [Crossref]
35. Fang WH, Li XD, Zhu H, et al. Resectable pancreatic ductal adenocarcinoma: Association between preoperative CT texture features and metastatic nodal involvement. *Cancer Imaging*. 2020;20(1):17. [Crossref]
36. Yan PF, Yan L, Hu TT, et al. The potential value of preoperative mri texture and shape analysis in grading meningiomas: A preliminary investigation. *Transl Oncol*. 2017;10(4):570-577. [Crossref]
37. Meyer HJ, Schob S, Hohn AK, Surov A. MRI texture analysis reflects histopathology parameters in thyroid cancer - A first preliminary study. *Transl Oncol*. 2017;10(6):911-916. [Crossref]
38. Liu S, Wen L, Hou J, et al. Predicting the pathological response to chemoradiotherapy of non-mucinous rectal cancer using pretreatment texture features based on intravoxel incoherent motion diffusion-weighted imaging. *Abdom Radiol (NY)*. 2019;44(8):2689-2698. [Crossref]
39. Beuzit L, Eliat PA, Brun V, et al. Dynamic contrast-enhanced MRI: Study of inter-software accuracy and reproducibility using simulated and clinical data. *J Magn Reson Imaging*. 2016;43(6):1288-1300. [Crossref]